Basal Melting and Potential Warm Water Intrusion Beneath Antarctic Ice Shelves

Shuang Wu[1,2], Tian Chang[1,2], Lu An[1,2]*, Rongxing Li[1,2]

[1]Center for Spatial Information Science and Sustainable Development Applications, Tongji University, 1239 Siping Road, Shanghai 200092, China – (2311686@tongji.edu.cn , ctzry@tongji.edu.cn, anlu2021@tongji.edu.cn , rli@tongji.edu.cn)
[2]College of Surveying and Geo-Informatics, Tongji University, 1239 Siping Road, Shanghai, China

Keywords: Antarctic Ice Shelves, Basal Melt, Warm Water Intrusion, Ice-Ocean Interaction.

Abstract

The intrusion of relatively warm ocean waters beneath Antarctic ice shelves is a key driver of basal melting and strongly influences ice-shelf stability. However, previous studies investigating warm-water pathways have largely relied on single-source datasets, such as ship-based Conductivity–Temperature–Depth (CTD) measurements, which are spatially sparse and limited to a few well-surveyed regions. Recent advances in multi-source remote sensing datasets provide new opportunities to address these limitations. In this study, a multi-source remote sensing–based framework is developed to identify potential pathways of relatively warm water intrusion beneath Antarctic ice shelves and to quantify the associated basal melting. The Moscow University Ice Shelf (MUIS) is used as a case study. Across the continental shelf, CTD observations, sub-ice-shelf bathymetry, and modeled ocean circulation are integrated to infer potential intrusion routes. At the ice-shelf front and base, EN4 reanalysis data are used to characterize seawater properties, while satellite-derived basal melt products are applied to analyze spatial and vertical patterns of basal melting. Results indicate that relatively warm water is mainly concentrated at depths of 300–500 m, coinciding with bathymetric depressions that facilitate its intrusion beneath MUIS. Enhanced basal melting occurs near the ice front and grounding line, primarily within the upper 0–500 m of the ice-shelf draft, with an average melt rate of ~6 m yr^{-1}. The proposed framework provides a transferable approach for investigating ocean-driven melting beneath Antarctic ice shelves.

1. Introduction

Antarctic ice shelves play a crucial role in regulating ice sheet dynamics and global sea-level rise by buttressing inland ice (Schodlok et al., 2016). Interactions between ice shelves and the underlying ocean, particularly basal melting driven by relatively warm water, are key factors influencing ice-shelf stability (Gwyther et al., 2020). Understanding the mechanisms and pathways of warm water intrusion beneath ice shelves is therefore essential for predicting ice-shelf response to climate change and assessing potential contributions to sea-level rise (Zhao et al., 2025).

Previous studies have examined warm water intrusion beneath specific Antarctic ice shelves. For instance, the Totten ice shelf has been investigated by combining radar-derived sub-ice topography with in situ Conductivity-Temperature-Depth (CTD) measurements at the ice front (Greenbaum et al., 2015; Rintoul et al., 2016). Similarly, the Shirase ice shelf has been analyzed using multi-source datasets, including multibeam echo sounder data, on-ice echo sounding data, hydrographic survey-based nautical charts, and ETOPO1, to reconstruct sub-ice topography, while shipborne CTD observations at the ice front were used to identify potential warm water intrusion pathways (Hirano et al., 2020). Although these studies offer important insights into basal melt dynamics at individual ice shelves, their applicability is constrained by the limited availability of field measurements, leaving most Antarctic ice shelves largely unexplored (Dow et al., 2018; Morlighem et al., 2020).

Recent advancements in oceanographic observations and high-resolution sub-ice topography provide new opportunities for more comprehensive investigations of ice–ocean interactions (Morlighem et al., 2020; Rignot et al., 2013). Shipborne CTD, seal-borne CTD (Roquet et al., 2013), Argo floats (Riser et al., 2016), and EN4 reanalysis data now offer vertical and spatial coverage of ocean temperature (Good et al., 2013), enabling identification of potential warm water pathways beneath ice shelves. High-resolution ice thickness and sub-ice topography from Bedmap3 allow precise determination of ice-shelf drafts and potential sub-ice conduits for warm water intrusion (Pritchard et al., 2025). In addition, satellite-derived basal melt products provide information on the spatial, temporal, and vertical distribution of ice-shelf melting (Paolo et al., 2023). Together, the integration of these multi-source datasets enables a physically constrained and systematic assessment of potential warm water intrusion and associated basal melt processes (Picton et al., 2023; Pritchard et al., 2012).

Building on these multi-source datasets, this study aims to identify potential pathways of relatively warm water intrusion beneath Antarctic ice shelves and to quantify the associated basal melting by developing a multi-source remote sensing–based framework. Using the Moscow University Ice Shelf (MUIS) as a case study, the framework is applied to two key regions: across the continental shelf, in situ CTD measurements, sub-ice-shelf bathymetry, and modeled ocean circulation are integrated to infer potential intrusion routes; at the ice-shelf front and base, EN4 reanalysis data are used to characterize seawater properties, while satellite-derived basal melt products are employed to analyze the spatial, temporal, and vertical patterns of basal melting on the ice shelf itself.

2. Study Area and Data

The MUIS is a narrow ice shelf about 220 km long, fringing the Sabrina Coast of Wilkes Land, East Antarctica (Figure 1). It is located east of the Totten ice shelf and west of Paulding Bay, serving as a major outlet for ice draining from the Aurora Subglacial Basin, one of the largest subglacial catchments in East Antarctica. The ice shelf occupies a relatively narrow coastal embayment, with a shallow continental shelf offshore and rugged

* Corresponding author

coastal topography inland. Its eastern section extends into the Dalton Tongue, which protrudes into the Southern Ocean.

To investigate potential pathways of warm water intrusion beneath the MUIS, we combined multi-source oceanographic observations, ice-shelf basal melt data, and sub-ice topography information. Oceanographic observations include shipborne CTDs from the World Ocean Database (temperature ±0.005–0.01 °C, salinity ±0.002–0.01 PSU, pressure ±0.5–1 dbar; https://www.ncei.noaa.gov/products/world-ocean-database) (Reagan et al., 2023), Argo floats (temperature ±0.002–0.01 °C, salinity ±0.01–0.03 PSU, pressure ±2 dbar; http://www.argo.ucsd.edu/) (Argo, 2000), and MEOP seal-borne CTDs (temperature ±0.02 °C, salinity ±0.05 PSU, pressure ±2 dbar, QC=1, indicating the measurements passed quality control checks; http://www.meop.net/) (Roquet et al., 2013). Additionally, the EN4 reanalysis (1960–2024, 1° × 1°; https://www.metoffice.gov.uk/hadobs/en4/download-en4-2-2.html) (Good et al., 2013) provides temperature and salinity fields generated by combining quality-controlled profiles with a background field derived from the previous month’s analysis and the 1971–2000 climatology, serving as a reference for the study region. Sub-ice topography and ice thickness data from Bedmap3 (500 m resolution; https://doi.org/10.5285/2d0e4791-8e20-46a3-80e4-f5f6716025d2) (Pritchard et al., 2024) have uncertainties of ±10–50 m for bed elevation and ±10–20 m for ice thickness. Regional ocean circulation was further examined using simulations from the Regional Ocean Modelling System (ROMS) to assess potential pathways of relatively warm water intrusion (Gwyther et al., 2014).

Basal melt rates were obtained from high-resolution (2010–2018, 500 m; https://doi.org/10.6075/J04Q7SHT) (Adusumilli et al., 2020b) and long-term (1992–2017, 1920 m; ITS_LIVE NSIDC-0792; https://doi.org/ 10.5067/SE3XH9RXQWAM) (Paolo et al., 2024) datasets to capture spatial and temporal variability. High-resolution melt rates were derived from CryoSat-2 altimetry, combining ice-shelf surface height changes, ice thickness, ice velocity, surface mass balance, and firn air content in a Lagrangian mass balance inversion to calculate depth-resolved meltwater fluxes. Long-term melt rates were produced by fusing ERS-1/2, Envisat, and CryoSat-2 radar altimetry, applying geophysical corrections, modeling firn air content and surface mass balance, and inverting ice thickness changes using mass conservation equations. The error of high-resolution melt rates for the Moscow University Ice Shelf is ±2.1 m/yr, while the long-term ITS_LIVE dataset has an error of ±4 m/yr.

In our analysis, these uncertainties were mitigated as follows: only quality-controlled observations (e.g., QC=1 for MEOP) were used; multiple observational sources were combined with spatial averaging to reduce random noise; and both high-resolution and long-term basal melt datasets were employed to capture consistent spatial and temporal trends. Although the datasets have inherent uncertainties, their magnitude is small relative to the spatial patterns of warm water intrusion pathways and ice-shelf basal melt features analyzed in this study. Therefore, these uncertainties do not affect the identification of major circulation pathways or the qualitative interpretation of warm water intrusion processes and basal melt drivers.

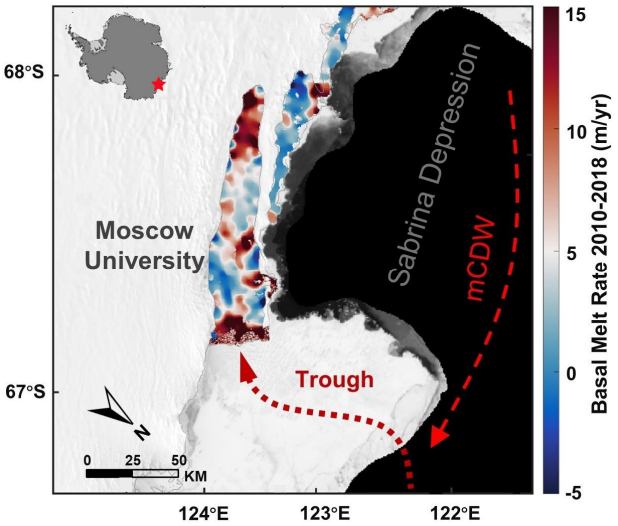

Figure 1 Study area showing the location of the MUIS along the Sabrina Coast, East Antarctica. The background is the 2008-2009 MODIS Mosaic of Antarctica, overlaid with mean basal melt rates of the three ice shelves for 2010-2018. Bright red dashed arrows indicate the circulation pathways of mCDW, while dark red dashed arrows show potential mCDW intrusion trough at the ice-shelf front.

3. Methodology and Results

We developed a multi-source remote sensing–based framework to systematically investigate two key aspects of ice–ocean interactions beneath Antarctic ice shelves: (1) potential pathways of relatively warm water intrusion, and (2) spatial, temporal, and vertical patterns of basal melting. The framework is designed to integrate complementary datasets that are largely publicly available, thereby reducing reliance on dense or site-specific field measurements. Using this framework, the analysis is applied to two regions: across the continental shelf, in situ CTD measurements are used to determine the depth and temperature of warm water, sub-ice-shelf bathymetry identifies topographic features that may facilitate intrusion, and modeled ocean circulation provides potential intrusion pathways; at the ice-shelf front and base, EN4 reanalysis data are used to characterize seawater properties, while satellite-derived basal melt products assess basal melting across spatial, temporal, and vertical dimensions (Figure 2).

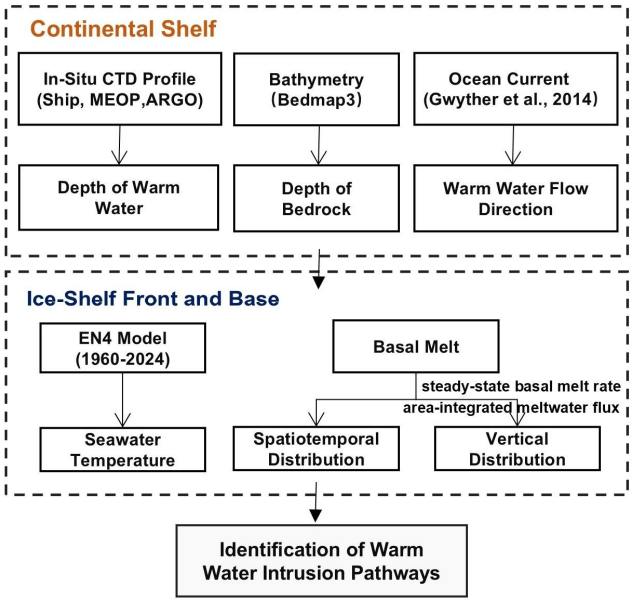

Figure 2. Framework for identifying potential pathways of warm water intrusion using multi-source remote sensing datasets.

3.1 Continental shelf

This section focuses on the continental shelf, where oceanographic and topographic conditions jointly control the access of relatively warm water to the sub–ice-shelf cavity. To constrain the presence, depth range, and potential routing of warm water toward the ice shelf, multiple complementary datasets are examined, including hydrographic observations, bathymetric features, and large-scale ocean circulation, which are analyzed separately in the following subsections.

3.1.1 Oceanographic Properties

The vertical distribution of ocean temperature near the MUIS was analyzed using in-situ CTD profiles. As shown in Figure 3, most of the water on the continental shelf exhibits temperatures above -1.8 °C, corresponding to the local surface freezing point. Potential warm water intrusion zones, indicated by brown boxes in Figure 3, show surface-layer temperatures (0-300 m) averaging -1.85 °C, with a maximum of -1.7 °C. Within the warm water layer (300-500 m), the average temperature reaches -1.10 °C, with a maximum of -0.20 °C, consistent with the depth range of mCDW reported by (Silvano et al., 2016). Across all depths, the mean temperature is -1.32 °C, with a maximum of -0.20 °C, indicating the presence of relatively warm water in this region.

3.1.2 Bathymetry

High-resolution sub-ice topography from Bedmap3 reveals that the MUIS region is underlain by complex bathymetry, including a deep continental slope (~2000 m), a relatively shallow continental shelf (~500 m), and a sub–ice-shelf trough reaching ~1000 m beneath the ice base (Figure 3). This configuration includes a retrograde bed slope (bed elevation increasing inland) that deepens toward the grounding line. Such a retrograde slope enhances the pressure gradient in a stratified water column, promoting the deeper penetration of relatively warm mCDW toward the ice-shelf base (Robel et al., 2021). Bathymetric troughs and deep channels on the continental shelf provide low-resistance conduits for mCDW to bypass the shelf break and access ice-shelf cavities, as observed in multiple Antarctic regions (Morlighem et al., 2020; Pattyn, 2018).

3.1.3 Ocean Circulation

Potential pathways of warm water intrusion are further supported by regional ocean circulation. Simulations from the ROMS (Gwyther et al., 2014) indicate that mCDW can access the northeastern edge of the MUIS at the continental shelf break and subsequently intrude beneath the ice shelf from the north (Figure 3). Persistent along-slope currents, together with mesoscale eddies generated by interactions between the Antarctic Circumpolar Current, coastal currents, and bathymetric features such as ridges and troughs, enhance poleward transport and lateral mixing of mCDW (Rintoul et al., 2001; Stewart and Thompson, 2015). These combined topographic and circulation features constitute the primary conditions favoring warm water intrusion beneath the MUIS, as they facilitate the delivery of heat to the ice-shelf base and determine the spatial distribution of basal melting (Moffat et al., 2009; St-Laurent et al., 2013).

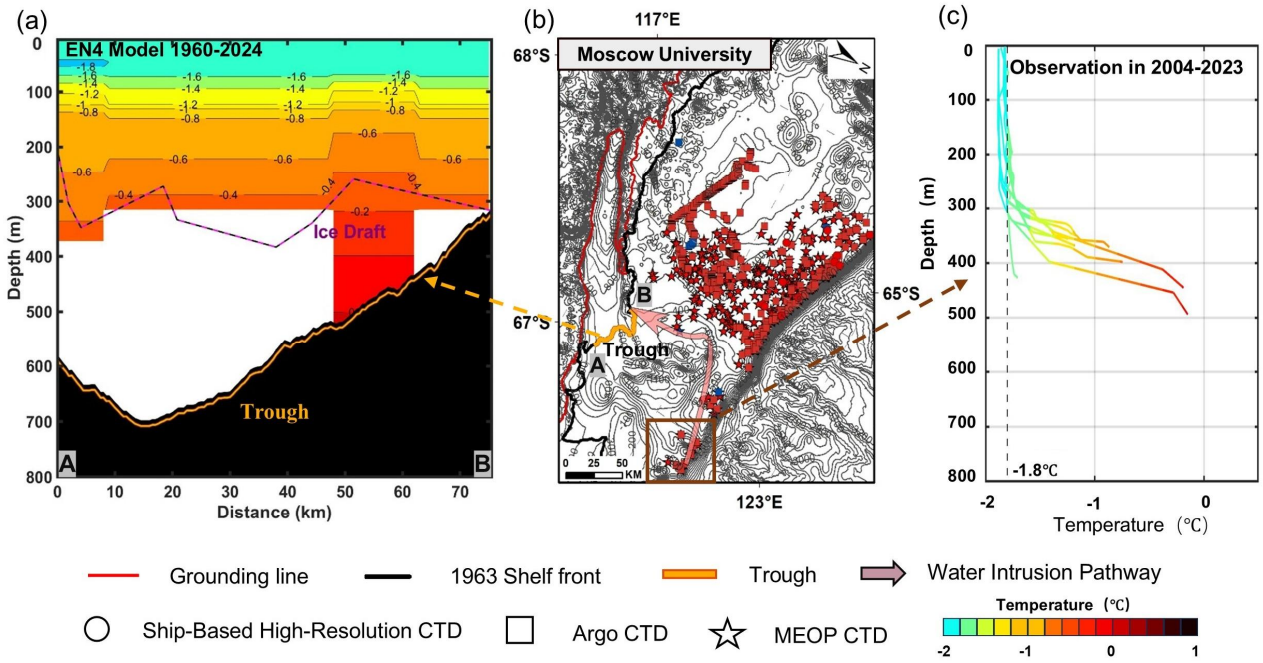

Figure 3. Ice–ocean interactions in the Moscow University ice shelves. (a) Vertical sections of modelled ocean temperature (EN4 reanalysis data) along transects aligned with the 1963 ice fronts; ice draft (dashed line) derived from Bedmap3. (b) Sub-ice-shelf cavity locations (orange lines) and in-situ temperature observations, with red indicating temperatures ⩾ -1.8 °C and blue indicating temperatures < -1.8 °C. Warm water intrusion pathways are highlighted in light red, with the Moscow University pathway based on literature. (c) Composite vertical temperature profiles within the boxed trough.

3.2 Ice Shelf Front and Base

To investigate potential warm water intrusion at the front of the MUIS, we examined bathymetric and ice draft characteristics together with seawater temperature observations from the EN4 reanalysis. Along the ice-shelf front (section AB), sub-ice topography ranges from 300 m to 700 m, while the ice draft is approximately 200–400 m, with a mean value around 300 m (Figure 3). The resulting sub-ice cavity spans depths of roughly 300–700 m, suggesting that mCDW at depths exceeding 300 m could access the ice-shelf cavity. Observed water temperatures below 400 m, typically 50–60 m above the ice base, exceed –0.4 °C, considerably warmer than the in situ freezing point (~–1.8 °C), further supporting the potential for mCDW intrusion. However, due to incomplete spatial coverage of the EN4 dataset, these observations provide only qualitative evidence of warm water presence beneath the ice shelf.

Spatial and temporal patterns of basal melting are shown in Figures 1 and Figure 4. The high-resolution 2010-2018 dataset (500 m) captures the spatial distribution of basal melt across the ice shelf, showing elevated melt near the ice front and grounding line, with an average rate of approximately 10 m yr^{-1}, while other regions of the ice shelf exhibit lower rates, averaging around 3 m yr^{-1}. Long-term variability was assessed using the ITS_LIVE NSIDC-0792 dataset (1992-2017, 1920 m resolution), which indicates that basal melt has generally remained at relatively high levels, with an annual mean of about 6 m yr^{-1}. Five-year moving averages reveal alternating trends: a decline from 1992 to 2000, an increase from 2000 to 2007, a decrease until 2013, and a final rise from 2013 to 2017, reflecting a dynamic basal melting environment potentially influenced by warm water intrusion.

To quantify the vertical basal melting of ice shelves, two key metrics were employed to capture distinct aspects of ice-shelf melt processes, following the approach of (Adusumilli et al., 2020a): the steady-state basal melt rate and the depth-resolved, area-integrated meltwater flux. The steady-state basal melt rate quantifies the melt rate required to maintain long-term ice-shelf mass balance, under the assumption that there is no net change in ice thickness. In contrast, the depth-resolved, area-integrated meltwater flux resolves the vertical distribution of melting across the ice-shelf base. The calculation of the steady-state basal melt rate is given by Equation (1).

$$w_{\text{steady}} = \frac{\langle M_s \rangle}{\rho_i} - \langle \nabla \cdot (H_i v) \rangle \quad (1)$$

where w_{steady}= steady-state basal melt rate, the basal melt required to maintain ice-shelf mass balance

M_s= time-averaged surface mass balance, calculated from the 2010–2018 mean of MERRA-2 Hybrid precipitation minus evaporation (Gelaro et al., 2017)

ρ_i= ice density, taken as 917 kg m^{-3} to convert surface mass balance to thickness units

$\langle \nabla \cdot (H_i v) \rangle$ = time-averaged divergence of ice flux, obtained from (Adusumilli et al., 2020a).

Following the approach of (Adusumilli et al., 2020a), basal melt rates from the high-resolution 2010-2018 dataset were first used to estimate the depth of the ice-shelf base relative to mean sea level, based on available ice thickness and surface elevation data. Melt rates at each grid cell were then aggregated into 30 m depth intervals, and meltwater flux for each interval was calculated in two steps: first, by summing the basal melt rates of all constituent grid cells, and second, by multiplying the summed melt rates by the total area of these grid cells. This procedure produced a depth-resolved profile of meltwater flux, directly reflecting the vertical structure of ice-shelf melting.

The vertical distribution of basal melting beneath the MUIS was assessed using the aforementioned metrics (Figure 4). Melting occurs throughout the ice-shelf base, with the highest meltwater flux concentrated in the shallow portion of the ice-shelf draft, around 200 m depth. Meltwater flux gradually declines with increasing depth, decreasing to less than half of the peak by 500 m and approaching negligible values below 1500 m. The steady-state basal melt curve closely follows the 95% confidence interval in the upper 0-300 m, while systematic deviations appear at greater depths. These results indicate that basal melting is predominantly concentrated in the upper 0-500 m of the ice-shelf draft, further supporting the potential influence of warm water intrusion.
.

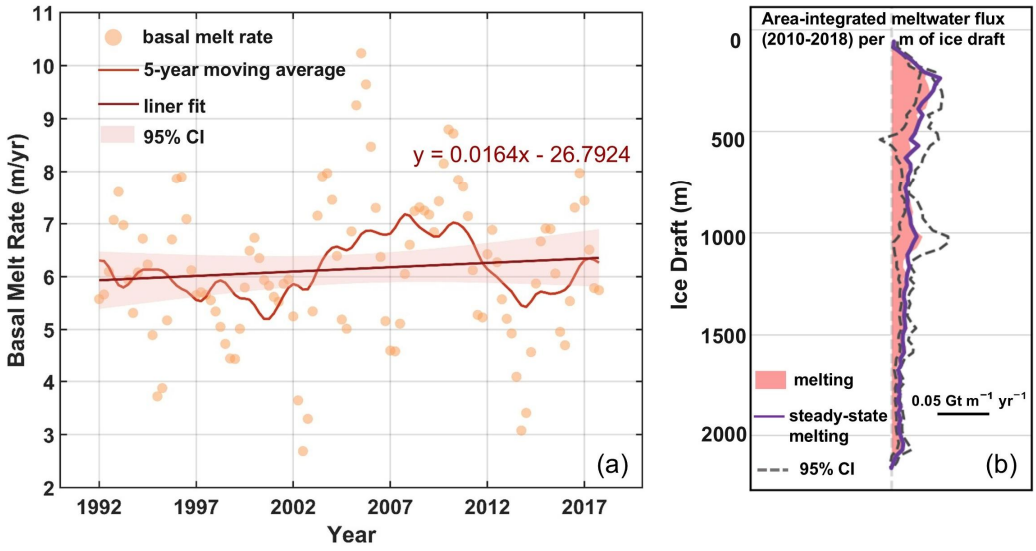

Figure 4. Basal melting of the Moscow University, and Holmes ice shelves. (a) Basal melt rates of the three ice shelves during 1992–2017 from the ITS_LIVE NSIDC-0792 dataset. (b) Depth-dependent, area-integrated meltwater fluxes for 2010–2018, illustrating the vertical distribution of melting across the ice-shelf bases. The horizontal axis scale is indicated by the solid black line. Shaded red regions denote mean values, and dashed lines represent the 95% confidence intervals. The purple lines indicate the hypothetical steady-state meltwater fluxes—that is, the fluxes required to maintain constant ice-shelf mass.

4. Conclusion

In this study, we developed a multi-source remote sensing–based framework to systematically identify potential pathways of relatively warm-water intrusion and to quantify the associated basal melting beneath Antarctic ice shelves, using the Moscow University Ice Shelf as a case study. By integrating oceanographic observations, sub-ice-shelf bathymetry, ocean circulation information, and satellite-derived basal melt products, the framework enables a coherent assessment of both warm-water access to the ice-shelf cavity and the resulting melt response. The results reveal that relatively warm water is concentrated at intermediate depths, aligned with bathymetric depressions that facilitate its intrusion, while enhanced basal melting occurs near the ice front and grounding line, primarily within the upper ice-shelf draft.

The proposed framework establishes a multi-source remote sensing–based framework for assessing warm-water intrusion and associated basal melting beneath Antarctic ice shelves. By progressively linking processes from the continental shelf to the ice-shelf cavity, it maintains physical consistency while allowing varying levels of constraint depending on regional data availability. Although data coverage remains heterogeneous, reanalysis products, bathymetry, and satellite-derived melt estimates provide first-order evidence where in situ observations are limited. Future integration of large-scale ocean state estimates (e.g., ECCO products) and expanding hydrographic datasets will further strengthen its regional applicability.

Acknowledgements

This work has been supported by the Natural Science Foundation of China (No.42394131), the Fundamental Research Funds for the Central Universities of China and Shanghai Pilot Program for Basic Research. We gratefully acknowledge the British Antarctic Survey for proving the Bedmap3 datasets used to determine ice thickness and sub-ice topography. We thank the Met Office for the EN4 ocean reanalysis data, as well as the World Ocean Database, Argo floats, and MEOP seal-borne CTD measurements for supplying essential temperature profiles. We also acknowledge the NASA GMAO team for the MERRA-2 atmospheric reanalysis. Finally, we sincerely appreciate the ITS_LIVE project and the CryoSat-2 mission for providing basal melt rate datasets. This study would not have been possible without the generous support and open access offered by these institutions and research teams.

References

Adusumilli, S., Fricker, H. A., Medley, B., Padman, L., and Siegfried, M. R. 2020a. Interannual variations in meltwater input to the Southern Ocean from Antarctic ice shelves. *Nature geoscience*, 13(9), 616-620. doi.org/10.1038/s41561-020-0616-z.

Adusumilli, S., Fricker, H. A., Medley, B. C., Padman, L., and Siegfried, M. R., 2020b. Interannual variations in meltwater input to the Southern Ocean from Antarctic ice shelves, UC San Diego Library Digital Collections. doi.org/10.6075/J04Q7SHT.

Argo, 2000. Argo float data and metadata from Global Data Assembly Centre (Argo GDAC), SEANOE. doi.org/10.17882/42182.

Dow, C. F., Lee, W. S., Greenbaum, J. S., Greene, C. A., Blankenship, D. D., Poinar, K., Forrest, A. L., Young, D. A., and Zappa, C. J. 2018. Basal channels drive active surface hydrology and transverse ice shelf fracture. *Science Advances*, 4(6), eaao7212. doi.org/10.1126/sciadv.aao7212.

Gelaro, R., McCarty, W., Suárez, M. J., Todling, R., Molod, A., Takacs, L., Randles, C. A., Darmenov, A., Bosilovich, M. G., and Reichle, R. 2017. The modern-era retrospective analysis for research and applications, version 2 (MERRA-2). *Journal of climate*, 30(14), 5419-5454. doi.org/10.1175/JCLI-D-16-0758.1.

Good, S. A., Martin, M. J., and Rayner, N. A. 2013. EN4: Quality controlled ocean temperature and salinity profiles and monthly objective analyses with uncertainty estimates. *Journal of Geophysical Research: Oceans*, 118(12), 6704-6716. doi.org/10.1002/2013JC009067.

Greenbaum, J., Blankenship, D., Young, D., Richter, T., Roberts, J., Aitken, A., Legresy, B., Schroeder, D., Warner, R., and Van Ommen, T. 2015. Ocean access to a cavity beneath Totten Glacier in East Antarctica. *Nature Geoscience*, 8(4), 294-298. doi.org/10.1038/NGE02388.

Gwyther, D., Galton-Fenzi, B., Hunter, J., and Roberts, J. 2014. Simulated melt rates for the Totten and Dalton ice shelves. *Ocean Science*, 10(3), 267-279. doi.org/10.5194/os-10-267-2014.

Gwyther, D. E., Kusahara, K., Asay-Davis, X. S., Dinniman, M. S., and Galton-Fenzi, B. K. 2020. Vertical processes and resolution impact ice shelf basal melting: A multi-model study. *Ocean Modelling*, 147(101569. doi.org/10.1016/j.ocemod.2020.101569.

Hirano, D., Tamura, T., Kusahara, K., Ohshima, K. I., Nicholls, K. W., Ushio, S., Simizu, D., Ono, K., Fujii, M., and Nogi, Y. 2020. Strong ice-ocean interaction beneath Shirase glacier tongue in east Antarctica. *Nature communications*, 11(1), 4221. doi.org/10.1038/s41467-020-17527-4.

Moffat, C., Owens, B., and Beardsley, R. 2009. On the characteristics of Circumpolar Deep Water intrusions to the west Antarctic Peninsula continental shelf. *Journal of Geophysical Research: Oceans*, 114(C5), doi.org/10.1029/2008JC004955.

Morlighem, M., Rignot, E., Binder, T., Blankenship, D., Drews, R., Eagles, G., Eisen, O., Ferraccioli, F., Forsberg, R., and Fretwell, P. 2020. Deep glacial troughs and stabilizing ridges unveiled beneath the margins of the Antarctic ice sheet. *Nature geoscience*, 13(2), 132-137. doi.org/10.1038/s41561-019-0510-8.

Paolo, F. S., Gardner, A. S., Greene, C. A., Nilsson, J., Schodlok, M. P., Schlegel, N.-J., and Fricker, H. A. 2023. Widespread slowdown in thinning rates of West Antarctic ice shelves. *The Cryosphere*, 17(8), 3409-3433. doi.org/10.5194/tc-17-3409-2023.

Paolo, F., Gardner, A., Greene, C., and Schlegel, N., 2024. MEaSUREs ITS_LIVE Antarctic Ice Shelf Height Change and Basal Melt Rates, Version 1, NASA National Snow and Ice Data Center Distributed Active Archive Center. doi.org/10.5067/SE3XH9RXQWAM.

Pattyn, F. 2018. The paradigm shift in Antarctic ice sheet modelling. *Nature communications*, 9(1), 2728. doi.org/10.1038/s41467-018-05003-z.

Picton, H. J., Stokes, C. R., Jamieson, S. S., Floricioiu, D., and Krieger, L. 2023. Extensive and anomalous grounding line retreat at Vanderford Glacier, Vincennes Bay, Wilkes Land, East Antarctica. *The Cryosphere*, 17(8), 3593-3616. doi.org/10.5194/tc-17-3593-2023.

Pritchard, H., Fretwell, P., Fremand, A., Bodart, J., Kirkham, J., Aitken, A., Bamber, J., Bell, R., Bianchi, C., Bingham, R., Blankenship, D., Casassa, G., Catania, G., Christianson, K., Conway, H., Corr, H., Cui, X., Damaske, D., Damn, V., ..., and Zirizzotti, A., 2024. BEDMAP3 - Ice thickness, bed and surface elevation for Antarctica - gridding products (Version 1.0), NERC EDS UK Polar Data Centre. doi.org/10.5285/2d0e4791-8e20-46a3-80e4-f5f6716025d2.

Pritchard, H., Ligtenberg, S. R., Fricker, H. A., Vaughan, D. G., van den Broeke, M. R., and Padman, L. 2012. Antarctic ice-sheet loss driven by basal melting of ice shelves. *Nature*, 484(7395), 502-505. doi.org/10.1038/nature10968.

Pritchard, H. D., Fretwell, P. T., Fremand, A. C., Bodart, J. A., Kirkham, J. D., Aitken, A., Bamber, J., Bell, R., Bianchi, C., and Bingham, R. G. 2025. Bedmap3 updated ice bed, surface and thickness gridded datasets for Antarctica. *Scientific data*, 12(1), 414. doi.org/10.1038/s41597-025-04672-y.

Reagan, J. R., Boyer, T. P., García, H. E., Locarnini, R. A., Baranova, O. K., Bouchard, C., Cross, S. L., Mishonov, A. V., Paver, C. R., Seidov, D., Wang, Z., and Dukhovskoy, D., 2023. World Ocean Atlas 2023, NOAA National Centers for Environmental Information. doi.org/10.25921/va26-hv25.

Rignot, E., Jacobs, S., Mouginot, J., and Scheuchl, B. 2013. Ice-shelf melting around Antarctica. *Science*, 341(6143), 266-270. doi.org/10.1126/science.1235798.

Rintoul, S. R., Hughes, C. W., and Olbers, D.: The Antarctic circumpolar current system, in: International geophysics, Elsevier, 271-XXXVI, 2001.

Rintoul, S. R., Silvano, A., Pena-Molino, B., Van Wijk, E., Rosenberg, M., Greenbaum, J. S., and Blankenship, D. D. 2016. Ocean heat drives rapid basal melt of the Totten Ice Shelf. *Science Advances*, 2(12), e1601610. doi.org/10.1038/nature12567.

Riser, S. C., Freeland, H. J., Roemmich, D., Wijffels, S., Troisi, A., Belbéoch, M., Gilbert, D., Xu, J., Pouliquen, S., and Thresher, A. 2016. Fifteen years of ocean observations with the global Argo array. *Nature Climate Change*, 6(2), 145-153. doi.org/10.1038/nclimate2872.

Robel, A. A., Wilson, E., and Seroussi, H. 2021. Layered seawater intrusion and melt under grounded ice. *The Cryosphere Discussions*, 2021(1-26. doi.org/10.5194/tc-16-451-2022.

Roquet, F., Wunsch, C., Forget, G., Heimbach, P., Guinet, C., Reverdin, G., Charrassin, J. B., Bailleul, F., Costa, D. P., and Huckstadt, L. A. 2013. Estimates of the Southern Ocean general circulation improved by animal-borne instruments. *Geophysical Research Letters*, 40(23), 6176-6180. doi.org/10.1002/2013GL058304.

Schodlok, M., Menemenlis, D., and Rignot, E. 2016. Ice shelf basal melt rates around A ntarctica from simulations and observations. *Journal of Geophysical Research: Oceans*, 121(2), 1085-1109. doi.org/10.1002/2015JC011117.

Silvano, A., Rintoul, S. R., and Herraiz-Borreguero, L. 2016. Ocean-ice shelf interaction in East Antarctica. *Oceanography*, 29(4), 130-143. doi.org/10.5670/oceanog.2016.105.

St-Laurent, P., Klinck, J. M., and Dinniman, M. S. 2013. On the role of coastal troughs in the circulation of warm Circumpolar Deep Water on Antarctic shelves. *Journal of Physical Oceanography*, 43(1), 51-64. doi.org/10.1175/JPO-D-11-0237.1.

Stewart, A. L. and Thompson, A. F. 2015. Eddy-mediated transport of warm Circumpolar Deep Water across the Antarctic Shelf Break. *Geophysical Research Letters*, 42(2), 432-440.

Zhao, C., Gladstone, R., Zwinger, T., Gillet-Chaulet, F., Wang, Y., Caillet, J., Mathiot, P., Saraste, L., Jager, E., and Galton-Fenzi, B. K. 2025. Subglacial water amplifies Antarctic contributions to sea-level rise. *Nature Communications*, 16(1), 3187. doi.org/10.1038/s41467-025-58375-4.